JOURNAL OF AIRCRAFT
Vol. 31, No. 5, Sept.–Oct. 1994

Preliminary Assessment of Tunnel Wall Interference in the NDA Cryogenic Wind Tunnel

Yutaka Yamaguchi,* Masahiro Yorozu,† Tadashi Sakaue,† and Teruo Saito‡
National Defense Academy, Yokosuka, Kanagawa 239, Japan

As the second stage of a preliminary cryogenic airfoil testing program, the test section interference of the National Defense Academy cryogenic tunnel was evaluated. A R4 airfoil model, which has the chord length of 12 cm and the aspect ratio of 0.5, was tested in the range of Mach number 0.5 to 0.75, and that of Reynolds number 7×10^6 to about 1.1×10^7. The experimental results were corrected with empirical wall interference correction methods, the Barnwell-Sewall method for sidewall boundary layers, and the Blackwell method for the top and bottom walls. This preliminary evaluation showed that the sidewall boundary layers dominate the tunnel wall interference of the present cryogenic tunnel, and there may be some possibility of utilizing the tunnel for performing two-dimensional airfoil tests if more precise wall interference parameters are obtained.

Nomenclature

b = tunnel width
C_p = pressure coefficient
$\bar{C}_p$ = equivalent pressure coefficient
c = chord length of the airfoil
c_n = section normal force coefficient
H = shape factor
M = local Mach number
M_c = corrected freestream Mach number
$\bar{M}_E$ = averaged experimental Mach number at the wall over the airfoil
$\bar{M}_T$ = averaged theoretical Mach number at the wall over the airfoil
M_∞ = tunnel freestream Mach number
$\bar{M}_\infty$ = equivalent Mach number
α = angle of attack
ΔM_B = blockage Mach number correction
ΔM_I = sequential Mach number correction
ΔM_W = sidewall Mach number correction
δ^* = sidewall displacement thickness

Subscripts
a = ambient condition
l = lower wall
u = upper wall

Introduction

THE Japanese National Defense Academy (NDA) started the preliminary study in 1981 for a high-speed continuous wind tunnel having relatively high Reynolds number capability to replace its old induction-type transonic wind tunnel. The cryogenic wind-tunnel concept has been proven as the best way to increase the Reynolds number capability of wind tunnels.[1–3] This concept can be applicable to a relatively small wind tunnel used for basic aerodynamic researches.

Although several methods were available for cooling the tunnel flow to cryogenic temperature and maintaining the total temperature in cryogenic range, the simplest and most efficient cooling method of injecting liquid nitrogen into the tunnel circuit was developed by the NASA Langley Research Center. In Japan, only two low-speed cryogenic tunnels at Tsukuba University[4] and a 0.1- × 0.1-m transonic cryogenic tunnel at National Aeronautical Laboratory (NAL)[5] had been constructed until 1984. We decided to adopt a cryogenic wind-tunnel concept of the similar NASA 0.3-m transonic cryogenic tunnel (TCT), and constructed a small two-dimensional high-speed cryogenic wind tunnel with a 0.06- × 0.30-m slotted wall test section as the Japanese fourth cryogenic tunnel in 1985. Since then, the calibration of the NDA tunnel and modification of the system have continued.[6–8]

In previous work[9] we had started to develop a technique of fabricating airfoil models for cryogenic wind-tunnel testing, and established one fabricating method for models as the second stage of our research work. Some experience was obtained with such a model for the cryogenic airfoil testing technique, and preliminary pressure distributions of an airfoil were measured as the first one of such a kind in Japan at cryogenic conditions. Several problems of the present cryogenic tunnel were also found.

The present tunnel has a very narrow test section width, and the allowable aspect ratio of airfoil model is less than 1.0 for our present model fabricating ability. Our present airfoil model has an aspect ratio of 0.5 and it is very interesting to know the interference effects of the test section walls to the pressure distributions of such a low aspect ratio model. This article describes the present status of the NDA cryogenic wind tunnel first, and then gives the preliminary airfoil testing results and wall interference effects of an airfoil model with an extremely low aspect ratio.

NDA Cryogenic Wind Tunnel

The NDA cryogenic wind tunnel is a closed-circuit tunnel with a centrifugal compressor driven by a 75-kW electric motor. The centerline dimensions are 5.5 m in the long direction and 1.2 m in the short direction.

The materials of the pressure shell are the stainless cast steel SCS13 for the contraction section and the high speed diffuser, and the stainless steel SUS304 for the other sections.

The tunnel has external insulation that mainly consists of 100 mm of formed urethane foam. The final vapor barrier is the zinc-plated steel of 0.3 mm thickness. No air purging system for insulation material is provided.

The test section is 0.06 m wide, 0.3 m high, and 1.0 m long, including the diffuser flap section. Both of the upper and lower walls have two slots of 3.6 mm width, and these slots

Presented as Paper 93-0421 at the AIAA 31st Aerospace Sciences Meeting and Exhibit, Reno, NV, Jan. 11–14, 1993; received June 16, 1993; revision received Jan. 19, 1994; accepted for publication Jan. 25, 1994.

*Professor, Department of Aerospace Engineering. Member AIAA.
†Graduate Student, Department of Aerospace Engineering.
‡Technical Assistant, Department of Aerospace Engineering.

Table 1 Major characteristics of NDA cryogenic tunnel

Type	Closed circuit, centrifugal compressor
Material of construction	SUS 304, SCS 13 stainless steel
Insulation	External
Cooling	Liquid nitrogen
Test gas	Nitrogen
Test section size (h, w, l)	0.3 × 0.06 × 0.72 m
Mach range	Up to 0.83
Contraction ratio	14:1
Stagnation pressure	Up to 1.77 bar
Stagnation temperature	108 K—ambient
Running time	Up to 100 min
Maximum Reynolds number/m	93 million
Drive motor	75 kW
Fan speed	Up to 2250 rpm
LN_2 tank volume	4.9 m^3

are spaced 33.6 mm from each other. The ratio of open area to the top or bottom wall area is about 9%. The sidewalls have no sidewall boundary-layer removal system.

A turntable system that we designed for our airfoil models is mounted on the test section side walls. An electric pulse motor drives this turntable. The angle of attack is changed up to ±15 deg in steps of 0.1 deg.

The test section and the turntable system are housed in the 711-mm-diam plenum chamber. The plenum chamber was mounted on a trolley to allow access to the test section.

The total temperature is controlled by regulating the flow rate of liquid nitrogen injected into the tunnel circuit. A dedicated digital proportional-integral-derivative (PID) controller is used for the control. The mean deviation of total temperature is ±0.5 K. The NASA Langley 0.3-m TCT and the NAL 0.1- × 0.1-m cryogenic tunnel are both operated with a temperature accuracy of ±0.1 K.[10,11] Therefore, the present total temperature control system should be also improved to have the accuracy of ±0.1 K for better experimental results.

The total pressure is also controlled by other digital PID controllers having signals from the pressure transducer for measuring the tunnel total pressure, and the total pressure deviation is maintained as ±0.1 kPa at steady-state operations by the present pressure control system. This accuracy is satisfactory, and is the same as other cryogenic tunnels.

The major characteristics of the NDA cryogenic tunnel are presented in Table 1. Operational tests of the present tunnel showed that cryogenic experiments at the lowest freestream Mach number M_∞ of 0.36 can be performed with the present control systems.

Cryogenic Airfoil Testing

Airfoil Model

In their previous work the authors tried to develop their own techniques for fabricating airfoil models used for cryogenic wind-tunnel testing.[9] The chosen airfoil section was R4.[12] This airfoil model was made of the stainless steel SUS 304, and has 24 pressure orifices on the upper surface, 17 orifices on the lower surface, 1 at the leading edge, and 1 at the trailing edge. A sketch of the airfoil section and the upper and lower surface pressure orifice layouts are presented in Fig. 1. These orifices were distributed on three lines; the midspan, and the right and left stations that are 2 mm apart from the midspan station. The model of Ref. 12 is equipped with pressure holes 0.3 mm in diam. Therefore, the same diameter was adopted for the present pressure orifices. The chord length is 12 cm. It was the minimum one for which the present technique could be applied to provide a total number of 43 pressure orifices. The aspect ratio of this model is only 0.5. This model was used in the present work.

Uncorrected Airfoil Characteristics

The pressure distribution of the R4 model was measured with two rotary fluid switches (type W02, Scanivalve Corp.),

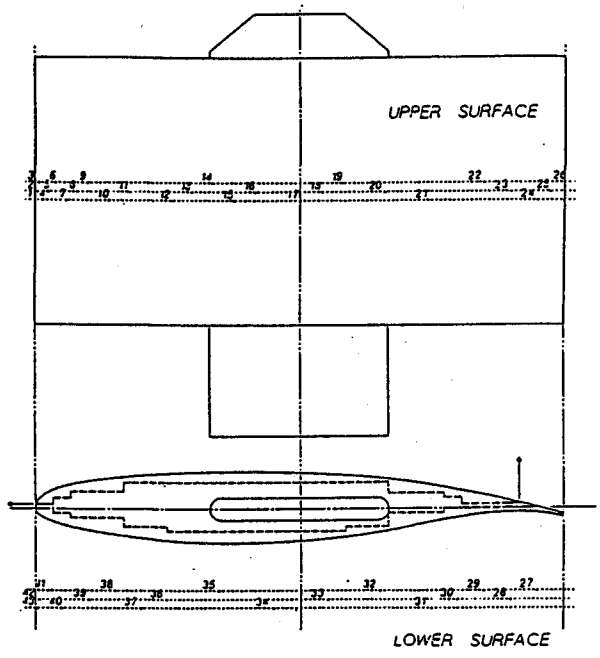

Fig. 1 Sketch of R4 airfoil model and pressure orifice locations.

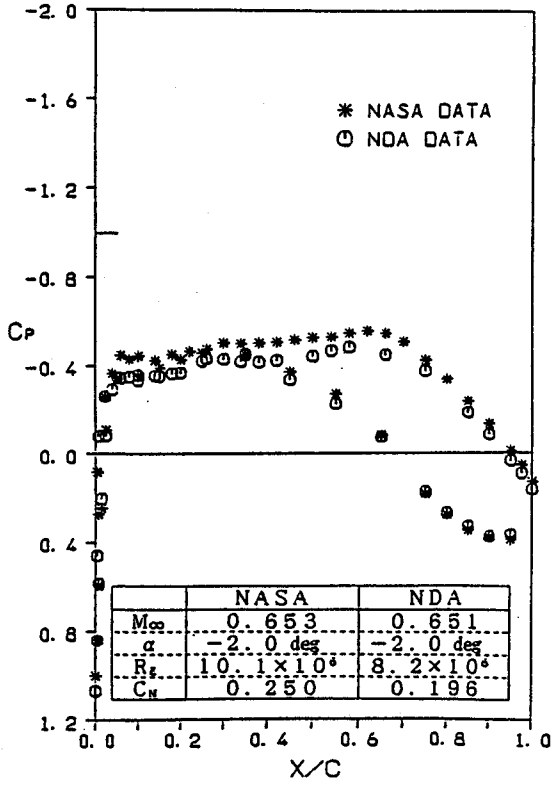

Fig. 2 Data from R4 airfoil at $\alpha = -2$ deg.

and two strain-gauge type pressure transducers. The ranges of the geometrical angle of attack and the nominal freestream Mach number were −3 to +3 deg, and 0.50 to 0.75, respectively. The total temperature of the tunnel flow was kept at 108 ± 0.5 K during the present experiment.

Figures 2 and 3 show the pressure distributions of the present model at the nominal $\alpha = -2$ and 0 deg, respectively. The freestream Mach number M_∞ is 0.65, and the Reynolds number based on the airfoil chord length is about 8.3 × 10^6. The boundary layer was free in the natural transition on the airfoil surface in the present experiment. Octagonal symbols indicate the present experimental pressure coefficients. For comparison, the asterisks represent data adopted from Ref. 13. They are of slightly higher Mach and Reynolds numbers

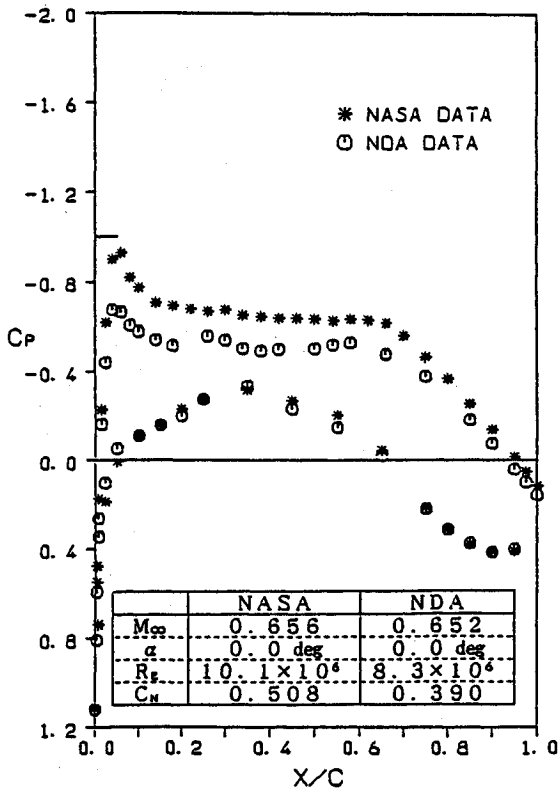

Fig. 3 Data from R4 airfoil at $\alpha = 0$ deg.

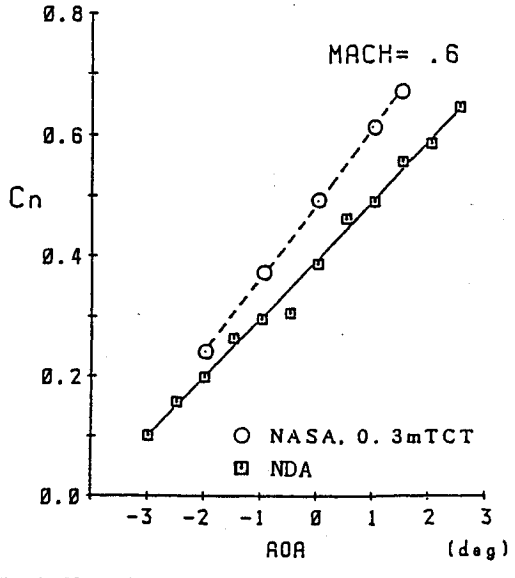

Fig. 4 Normal force coefficient curve of R4, $M_\infty = 0.6$.

than those of NDA. Neither the present data nor the data from Ref. 13 are corrected for the test section wall interference effects. Strictly speaking, corrected data should be used for comparison, because a wind tunnel influences aerodynamic data of a model tested in it with its particular effects. But, as a preliminary step, the present uncorrected data were compared with those of Ref. 13, which are considered as the most reliable experimental data of the R4 airfoil.

The pressure distribution data from the present experiment and Ref. 13 are in reasonable agreement in the negative angle-of-attack range as shown in Fig. 2. But, at higher angle of attack and higher Mach number, significant discrepancies appear in the pressure distributions.

Figure 4 shows c_n at $M_\infty = 0.6$. The present c_n—shown as symbols of squares—were calculated by integrating the experimental pressure distributions. The circles are also data adopted from Ref. 13. From this figure, it is clearly shown that the present experimental results were more influenced by the tunnel walls than those of Ref. 13.

Preliminary Wall Interference Corrections

Research on wall interference effects up to transonic speeds have indicated that a correction to the freestream Mach number and angle of attack is sufficient for a large number of flows.[14] As another matter of importance, Barnwell showed that the sidewall boundary-layer effect should be considered for two-dimensional airfoil tests.[15]

Sudani et al.[16] studied the sidewall effects in the two-dimensional transonic airfoil testing with airfoil models of several aspect ratios by the flow visualization techniques. They pointed out that an aspect ratio of a model for a two-dimensional test should be higher than 1.5 to avoid strong sidewall effects on the airfoil pressure distribution. As mentioned before, the present model has an aspect ratio of 0.5. According to Ref. 16, the value may be too low for an airfoil test, but it is interesting to know if the test results of such a low aspect ratio model are correctable.

Two types of the tunnel test section wall interference effects were separately considered in this article. One is the sidewall boundary-layers effect, and the other is the top and bottom wall effects. The pressure distributions in free air field were computed by the FLO54 program, which was developed by Jameson and Schmidt. Although it solves inviscid transonic airfoil flows with the unsteady Euler equations, it may work for the present preliminary purpose of assessing the approximate magnitude of the interference. Then, the experimental pressure distributions were compared with the calculated ones. In computations, the angle of attack was varied to produce the experimental value of c_n, while the Mach number was fixed.

Estimation of the Sidewall Effects

As for the sidewall boundary-layer corrections, Barnwell[15] developed a method accounting for the effect of the attached sidewall boundary-layer thickness at subsonic conditions. Sewall[17] also extended the Barnwell's method to transonic conditions. Murthy[18] developed a method to account for the airfoil aspect ratio, which was neglected in both of the Barnwell and Sewall correction methods. It is shown in Ref. 18 that the Barnwell and Sewall correction methods tend to overcorrect the boundary-layer effects when the model aspect ratio is greater than 1. Sudani et al. also applied the Murthy's method to their experimental data, which are of the aspect ratios of 1.2, 1.5, and 2.5, and concluded that their corrected data agreed well with those of other wind tunnels. Therefore, the Murthy method should be adopted when the aspect ratio is greater than 1. However, the aspect ratio of the present airfoil model is 0.5, and it is sufficiently lower than the critical value of 1.0. Therefore, the method of Barnwell-Sewall was adopted for this study.

According to the theory,[17] the relationship between the measured M_∞ and an interference-free $\bar{M}_\infty$ is given as

$$M_\infty - \bar{M} \simeq \frac{3M_\infty}{2 + M_\infty^2}\left(2 + \frac{1}{H} - M_\infty^2\right)\frac{\delta^*}{b} \qquad (1)$$

and the relationship between C_p and $\bar{C}_p$ is

$$\bar{C}_p = (\tilde{\beta}/\sqrt{1 - \bar{M}_\infty^2})C_p \qquad (2)$$

where

$$\tilde{\beta} = \{1 - M_\infty^2 + (2\delta^*/b)[2 + (1/H) - M_\infty^2]\}^{1/2} \qquad (3)$$

Applying this theory to the correction of airfoil pressure distributions, δ^* and H of the boundary layer on the tunnel

sidewalls must be known. The side wall boundary layer on the present test section has not yet been measured at the cryogenic conditions because we have not been able to develop a traverse equipment that can be housed in the present small plenum chamber and still works properly in the cryogenic environment.

The sidewall boundary-layer measurements for low speeds at the ambient condition were only performed in the early stage of the tunnel calibration test.[7] The measured maximum thickness of the boundary layer was about 12 mm at a unit Reynolds number of 2.3×10^6. Therefore, the displacement thickness was about 1.8 mm. Although such data are not exactly the same as the present sidewall configuration, it is simply assumed that the sidewall boundary layer behaves as a flat plate turbulent boundary layer, and the boundary-layer thickness at the cryogenic condition δ can be estimated by multiplying one at the ambient condition δ_a, with a factor of the one-fifth power[19] of the ratio of unit Reynolds numbers between the ambient and cryogenic conditions. The shape factor at the cryogenic condition H is also assumed to have the same value as that at the ambient condition, about 1.6. Thus, utilizing the ambient values, the estimated δ^* at the cryogenic condition were about 1 mm, and the estimated Mach number correction due to the sidewall boundary layers was about -0.03 in the freestream Mach number range of up to 0.75.

Table 2 shows the results of the Mach number correction due to the sidewall boundary layers ΔM_W and the correction factor of C_p, FA $(=\bar{C}_p/C_p)$. Figures 5 and 6 show examples of the measured and corrected pressure distributions, respectively. The experimental Mach number was 0.70, and the Reynolds number was 9.8×10^6. The symbols (asterisks and triangles) of Fig. 5 are the measured C_p, and those of Fig. 6 are $\bar{C}_p$. The solid lines are the computed distributions at the indicated Mach numbers, and calculated as mentioned

Table 2 Correction parameters due to side wall boundary layers

M_∞	ΔM_W	FA[a]
0.75	−0.030	1.0250
0.70	−0.030	1.0274
0.65	−0.030	1.0300
0.60	−0.030	1.0322
0.55	−0.030	1.0345
0.50	−0.030	1.0366

[a]FA = Correction Factor of C_p, C_p/C_p.

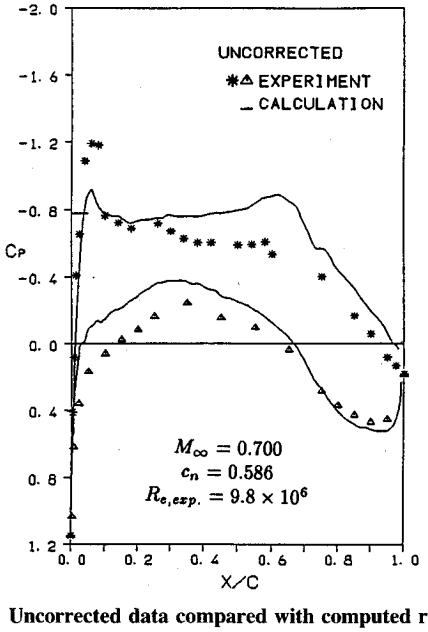

Fig. 5 Uncorrected data compared with computed results.

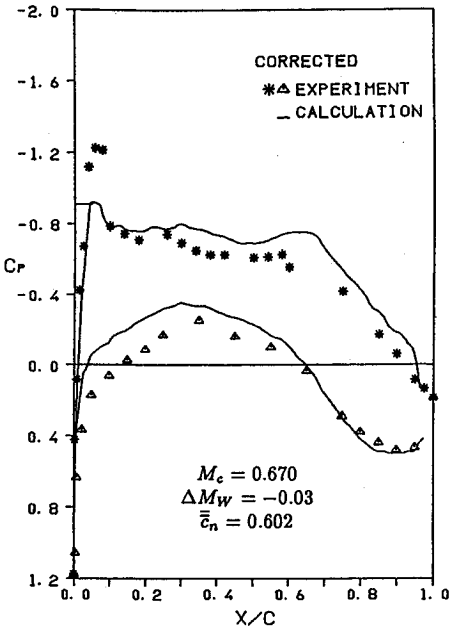

Fig. 6 Corrected data for sidewall boundary layers compared with computed results, $M_\infty = 0.700$, $\Delta M_W = -0.030$.

before. Although quantitative discrepancy still exists, the agreement between the corrected experimental data and the computed ones was improved by this correction. In the next section, the blockage correction will be considered.

First-Order Blockage Correction

For designing slotted wall test sections for two-dimensional wind tunnels, a design method for minimizing the blockage and streamline curvature was also developed by Barnwell.[20] However, the present test section was not based on such a theory, and may be far from the optimum design.

The semiheight of the present test section is 150 mm, and the slot width is 3.6 mm. The slot spacing is 33.6 mm. Following Barnwell's procedure,[20] the openness ratio is defined as that of the slot width to the slot spacing. The average openness ratio in the vicinity of the model is 0.11. The approximate value of the wall boundary condition coefficient k was calculated by Eq. (6) of Ref. 20, and it is found that k has a value of 0.47. The blockage-free value of k is 1.18, and the tunnel test section having k less than 1.18 is considered to be close to an open jet. Again, from Fig. 3 of Ref. 20, the present test section may behave like an open jet, rather than a closed one. The Mach number correction was found to be a very small value, less than -0.001.

To provide corrections for the ventilated wall interference effects, other methods utilizing experimental wall pressure data have been proposed for the transonic airfoil tests. Such empirical methods for the two-dimensional test have been published by Blackwell,[21] Mockry and Ohman,[22] and Sawada.[23] These methods utilize the wall pressure distributions measured with pressure rails on the tunnel top and bottom walls. Both methods of Refs. 22 and 23 can provide the first-order corrections for both Mach number and angle of attack on airfoils, and require detailed wall pressure distributions. On the other hand the Blackwell's method gives only Mach number correction, but simply needs the wall pressure distributions over the region of the airfoil.

Both the top and bottom walls of the present tunnel have 10 pressure orifices, with intervals of 5 cm. Although four orifices on the top and three on the bottom walls were available, they are over the region of the airfoil. Therefore, the Blackwell's method was adopted to evaluate the preliminary blockage effect.

In Blackwell's method, an airfoil was represented with a point doublet located at the quarterchord point, and the

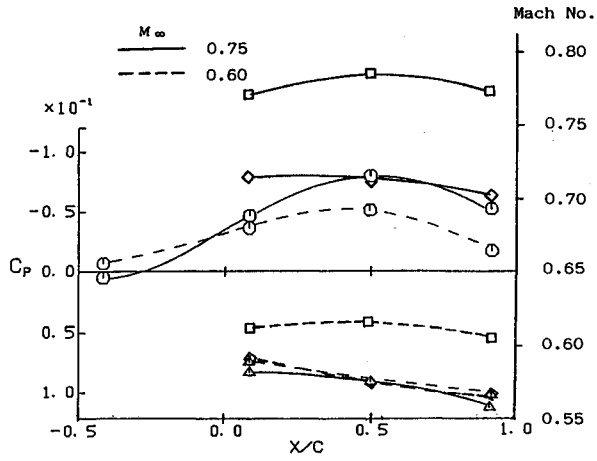

Fig. 7 Wall pressure distribution, $\alpha = +1$ deg.

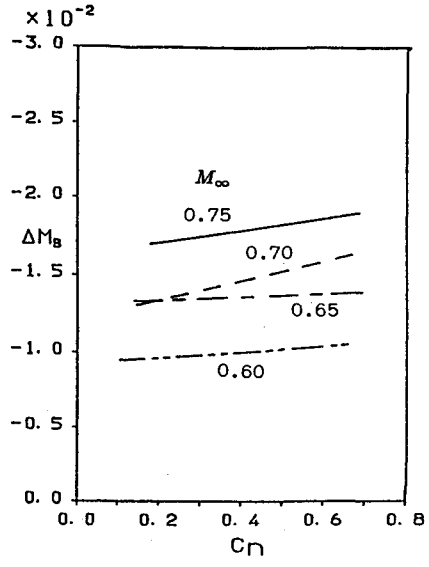

Fig. 8 Variation of blockage Mach number correction with normal force coefficient for R4.

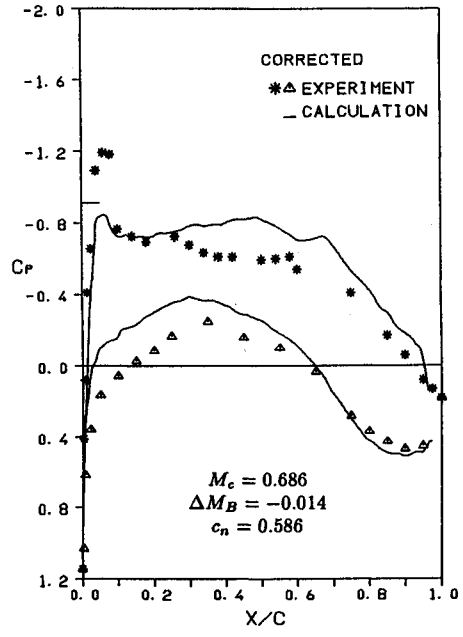

Fig. 9 Data corrected only for blockage compared with computed results, $M_\infty = 0.700$, $\Delta M_B = -0.014$.

blockage correction is assumed to be constant over the length of the airfoil. Therefore, the averaged perturbation velocity for the correction is obtained by integrating the local perturbation velocity over the airfoil chord. The blockage correction is given by Eqs. (1), and (6–8) of Ref. 21.

ΔM_B is calculated by

$$\Delta M_B = \bar{M}_E - \bar{M}_T \tag{4}$$

$\bar{M}_E$ is calculated by the following equation[21]:

$$\bar{M}_E = \frac{1}{c}\int_0^c \frac{M_u + M_l}{2}\,dx \tag{5}$$

and $\bar{M}_T$ is also calculated by Eqs. (6) and (7) of Ref. 21.

Figure 7 shows examples of the measured top and bottom wall pressure distribution and corresponding wall Mach number ones for R4 at the nominal angle of attack of +1 deg. The octagonal symbols indicate the top wall pressure coefficients, and the triangular ones indicate the bottom wall pressure coefficients. Square and diamond symbols indicate the Mach numbers calculated from the pressure distributions on the top and bottom walls, respectively. The fitted solid and dotted lines are of $M_\infty = 0.75$ and 0.6, respectively. In this figure, the airfoil leading and trailing edges are located at $x/c = 0.0$ and 1.0, respectively.

$\bar{M}_E$ has been calculated by integrating Mach number distributions, which are similar to Fig. 7, through Eq. (5). ΔM_B have been obtained by Eq. (4). Figure 8 shows ΔM_B vs c_n. Those results are one order higher than that by the Barnwell's method. It may be due to the fact that the present top and bottom walls have the thickness of 30 mm, and do not satisfy the wall condition of zero thickness for the theory. In addition, the model location is near the aft-end of the test section. This also violates one of the conditions of the theory. Therefore, we will use the empirical results for evaluating the blockage effects.

ΔM_B curves slightly depend on c_n at lower freestream Mach numbers, and such a tendency becomes more evident at higher Mach numbers. In Blackwell's[21] method, the effect of airfoil lift is eliminated by averaging the upper and lower wall values as Eq. (5), and the correction should be invariant with c_n. From the present results, more precise pressure measurements at the wall over the region of the model should be performed for more accurate evaluation. But, the present results as shown in Fig. 8 were considered to be adequate for the preliminary wall interference assessment.

Figure 9 shows an example of the only blockage corrected pressure distribution (asterisks and triangles) of the R4 airfoil with the computed freestream distribution (the solid line), which were again calculated as the same manner as in the sidewall correction. Although the Mach number correction varies from -0.01 up to -0.02, depending on the freestream Mach number, the agreement between the blockage corrected experimental pressure distribution and the computed one is not better than that of the sidewall correction as seen in Fig. 9. In addition, the computed pressure distributions were relatively insensitive to the blockage correction. These facts indicate that the sidewall boundary layers dominate the tunnel wall interferences, and that it is most important to correct the sidewall effects for the present cryogenic wind tunnel.

The four-wall interference assessment was also attempted by combining the corrections for the sidewall boundary layer and the top and bottom wall interference. The employed procedure was a kind of sequential procedure. In that procedure, the sidewall corrections were made first, and then the top and bottom wall pressure distributions were also corrected by the Barnwell-Sewall method to get the boundary-layer effect-free Mach number distributions on the walls. Finally, the Blackwell's correction was applied to the first corrected results.

Figure 10 shows the sequentially corrected pressure distribution. The solid line is the computed distribution producing

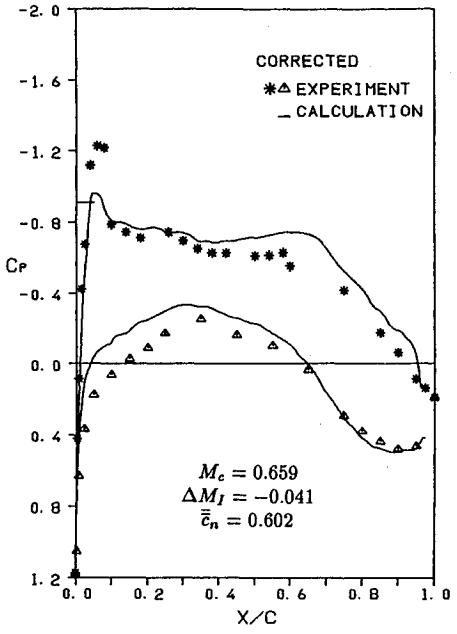

Fig. 10 Corrected data for sidewalls and blockage compared with computed results, $M_\infty = 0.700$, $\Delta M_W = -0.030$, $\Delta M_B = -0.011$.

$c_n = 0.602$ at $M_c = 0.659$. The equivalent blockage correction is -0.011, which is a little smaller than the uncorrected one. Comparing Figs. 5, 6, and 10, it is clear that the sequential correction produces the further improved agreement between the corrected data and the computed ones. However, the quantitative discrepancy still exits between them. This discrepancy may be partly due to the roughly approximate parameters used for the empirical corrections, and partly due to the fact that the employed computational code did not include the airfoil boundary-layer effect. The corrected results indicate that the correction is in the right direction, and it is expected that the corrections on the experiment will become more accurate if the better correction parameters are obtained. Therefore, further experimental works will be needed to get better correction parameters for the present cryogenic wind tunnel, and the viscous effects should be included in the computational code.

Concluding Remarks

The Barnwell-Sewall method for the boundary-layer effects and the Blackwell method for the solid blockage were applied to the R4 airfoil pressure distributions obtained at the NDA cryogenic wind tunnel. Although the empirical data required for applying the correction methods were very coarse ones, the preliminary wall interference magnitudes were obtained. The comparison of the corrected experimental data and the computed ones indicated that the Barnwell-Sewall method is very useful to evaluate the airfoil pressure distributions in the present tunnel, and consequently, that there may be some possibility of obtaining the airfoil characteristics from a model of a low aspect ratio as low as 0.5 in the NDA small cryogenic tunnel by applying the two correction methods together, and further experimental and numerical studies should be performed to validate this expectation.

Acknowledgments

The authors wish to thank Robert A. Kilgore at CES-Hampton for his invaluable advice on the cryogenic wind-tunnel technology. The authors also wish to thank Murthy at NASA Langley Research Center, and Hideo Sawada and his colleagues at the National Aerospace Laboratory for their advice on the wall interference corrections.

References

[1]Kilgore, R. A., Adcock, J. B., and Ray, E. J., "Flight Simulation Characteristics of the Langley High Reynolds Number Cryogenic Transonic Tunnel," *Journal of Aircraft*, Vol. 11, No. 10, 1974, pp. 593–600.

[2]Baals, D. D., "High Reynolds Number Research," NASA CP-2009, 1977.

[3]Kilgore, R. A., "Advanced Experimental Techniques for Transonic Wind Tunnels (unpublished)," Lecture Notes of Lecture Series presented at the National Defense Academy, 1987.

[4]Yoshizawa, Y., "Cryogenic Variable Pressure Wind Tunnel," *Journal of the Japan Society for Aeronautical and Space Sciences*, Vol. 31, No. 351, 1983, pp. 190–196 (in Japanese).

[5]Takashima, K., Sawada, H., Aoki, T., and Kayaba, S., "Trial Manufacture of NAL 0.1 m × 0.1 m Transonic Cryogenic Wind Tunnel," National Aerospace Laboratory, NAL TR-910, Aug. 1986 (in Japanese).

[6]Yamaguchi, Y., Kaba, H., Yoshida, S., and Kuribayashi, N., "Preliminary Test Results of NDA Cryogenic Wind Tunnel and Its System," Society of Automotive Engineers, SAE TP 881449, Oct. 1988.

[7]Yamaguchi, Y., Kaba, H., Yoshida, S., Kuribayashi, N., Nakauchi, Y., and Saito, T., "Instrumentation and Operation of NDA Cryogenic Wind Tunnel," *Proceedings of ICIASF'89*, IEEE, 1989, pp. 460–469.

[8]Yamaguchi, Y., Kaba, H., Kuribayashi, N., and Nakauchi, Y., "Characteristics of a Cryogenic Wind Tunnel at National Defense Academy; Tunnel Characteristics at Ambient and Cryogenic Temperatures," *Journal of the Japan Society for Aeronautical and Space Sciences*, Vol. 38, No. 441, 1990, pp. 559–565 (in Japanese).

[9]Yamaguchi, Y., Nakauchi, Y., Yorozu, M., and Saito, T., "Preliminary Airfoil Testing Experience in the NDA Cryogenic Wind Tunnel," *Proceedings of ICIASF'91*, IEEE, 1991, pp. 223–230.

[10]Thibodeaux, J. J., and Balakrishina, S., "Automatic Control of a 0.3 m Cryogenic Test Facility," *Journal of Guidance Control and Dynamics*, Vol. 4, No. 4, 1981, pp. 428–432.

[11]Sawada, H., Sekine, H., Aoki, T., Takashima, K., Takatsuka, T., Wakai, H., and Hastutori, K., "Automatic Control of NAL Cryogenic Wind Tunnel," *Proceedings of the 17th Annual Meeting of the Japan Society for Aeronautical and Space Sciences*, 1986, pp. 159, 160 (in Japanese).

[12]Jenkins, R. V., "R4 Airfoil Data Corrected for Side Wall Boundary-Layer Effects in the Langley 0.3-Meter Transonic Cryogenic Tunnel," NASA TP-2565, May 1986.

[13]Jenkins, R. V., Johnson, W. J., Jr., Hill, A. S., Mueller, R., and Redeker, G., "Data from Tests of an R4 Airfoil in the Langley 0.3-Meter Transonic Cryogenic Tunnel," NASA TM-85739, Sept. 1984.

[14]Nixon, D., *Transonic Aerodynamics*, Vol. 81, Progress in Astronautics and Aeronautics, AIAA, New York, 1981, pp. 189–238.

[15]Barnwell, R. W., "Similarity Rule for Sidewall Boundary-Layer Effect in Two-Dimensional Wind Tunnels," *AIAA Journal*, Vol. 18, No. 9, 1980, pp. 1149–1151.

[16]Sudani, N., Sato, M., Kanda, H., and Matsuno, K., "Flow Visualization Studies on Sidewall Effects in Two-Dimensional Transonic Airfoil Testing," AIAA Paper 93-0090, Jan. 1993.

[17]Sewall, W. G., "Effects of Sidewall Boundary Layers in Two-Dimensional Subsonic and Transonic Wind Tunnels," *AIAA Journal*, Vol. 20, No. 9, 1982, pp. 1253–1256.

[18]Murthy, A. V., "Effect of Aspect Ratio on Sidewall Boundary-Layer Influence in Two-Dimensional Airfoil Testing," NASA CR-4008, Sept. 1986.

[19]Schlichting, H., "Boundary Layer Theory," 7th ed., McGraw-Hill, New York, 1979, pp. 636–638.

[20]Barnwell, R. W., "Design and Performance Evaluation of Slotted Walls for Two-Dimensional Wind Tunnel," NASA TM-78648, Feb. 1978.

[21]Blackwell, J. A., Jr., "Wind-Tunnel Blockage Correction for Two-Dimensional Transonic Flow," *Journal of Aircraft*, Vol. 16, No. 4, 1979, pp. 256–263.

[22]Mokry, M., and Ohman, L. H., "Application of the Fast Fourier Transform to Two-Dimensional Wind Tunnel Wall Interference," *Journal of Aircraft*, Vol. 17, No. 6, 1980, pp. 402–408.

[23]Sawada, H., "A General Correction Method of the Interference in 2-Dimensional Wind Tunnel with Ventilated Walls," *Transactions of the Japan Society for Aeronautical and Space Sciences*, Vol. 21, No. 52, 1978, pp. 57–68.